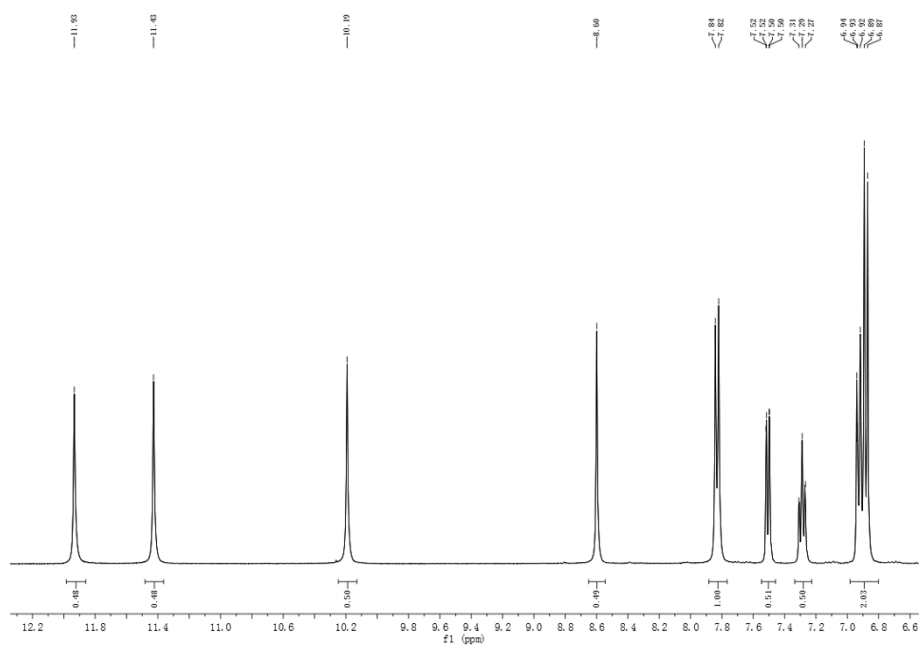


# A highly selective turn-on and reversible fluorescent chemosensor for Al<sup>3+</sup> detection based on novel salicylidene Schiff base-terminated PEG in pure aqueous solution

Liping Bai, Yuhang Xu, Guang Li\*, Shuhui Tian, Leixuan Li, Farong Tao, Aixia Deng, Shuangshuang Wang and Liping Wang\*

<sup>1</sup> School of Materials Science and Engineering, Liaocheng University, Liaocheng 252059, China

\* Correspondence: lglzsd@126.com (G.L.); wangliping5@163.com (L.W.); Tel: +86-635-823-0919



**Figure S1.** <sup>1</sup>H NMR spectrum of BAB in DMSO-*d*<sub>6</sub>.

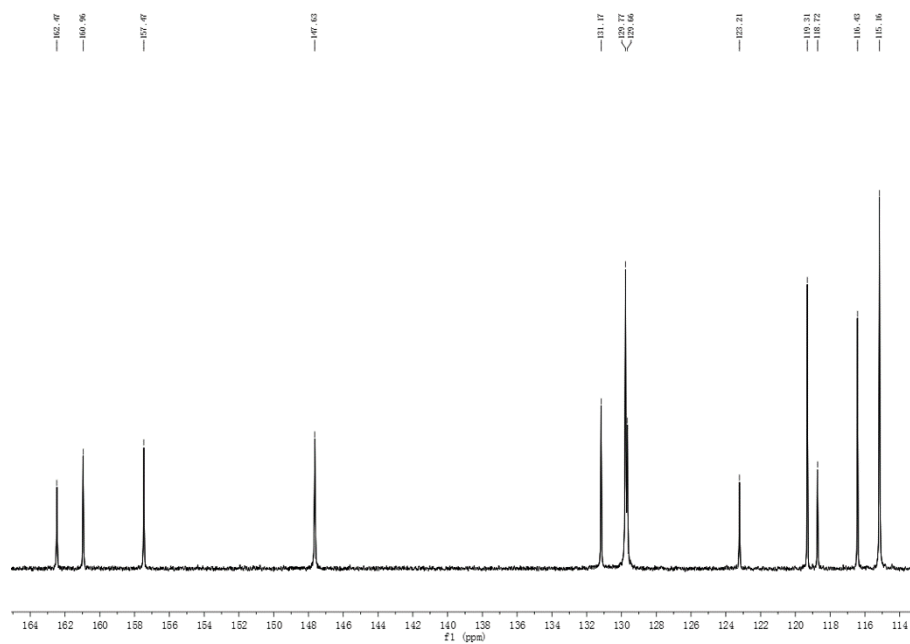


**Figure S2.**  $^{13}\text{C}$  NMR spectrum of BAB in  $\text{DMSO-}d_6$ .

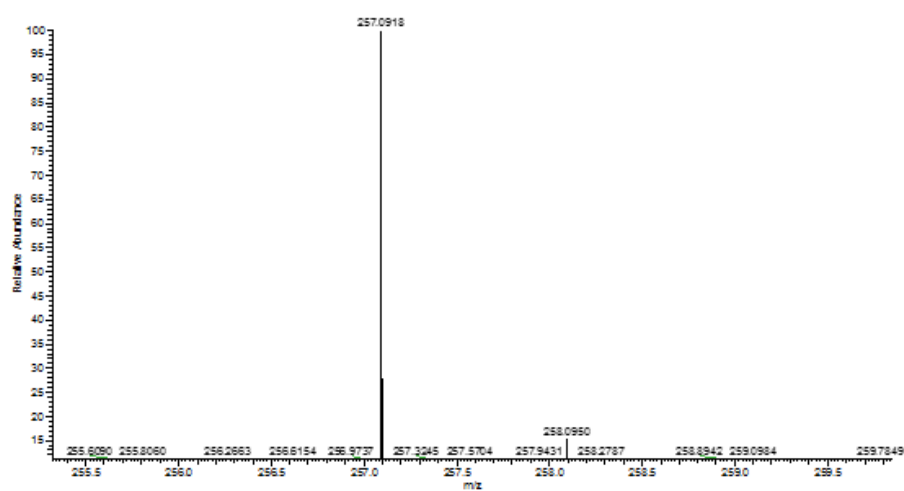


**Figure S3.** ESI-MS spectrum of BAB.

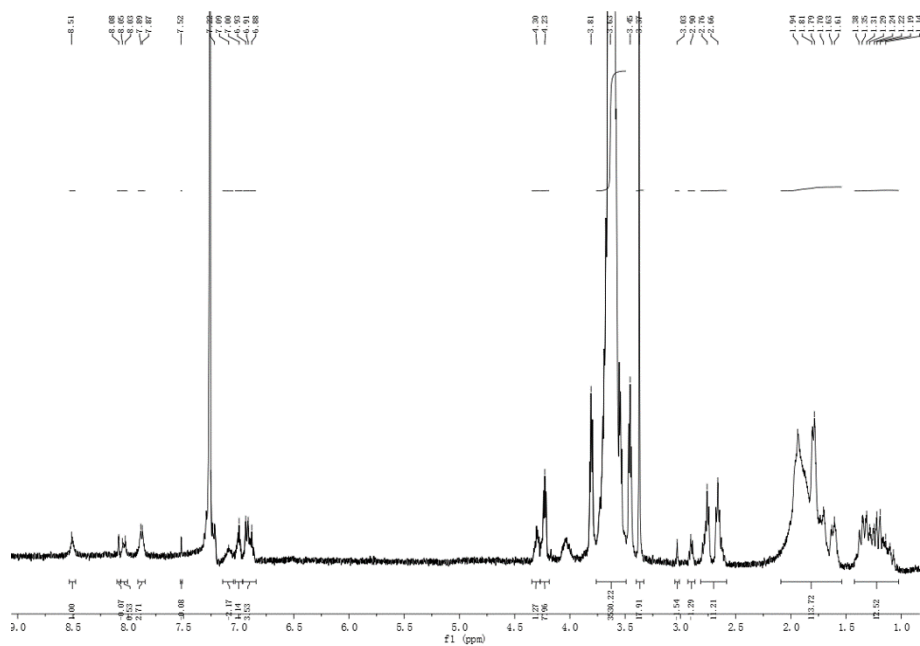


**Figure S4.**  $^1\text{H}$  NMR spectrum of PEGBAB in  $\text{CDCl}_3$ .

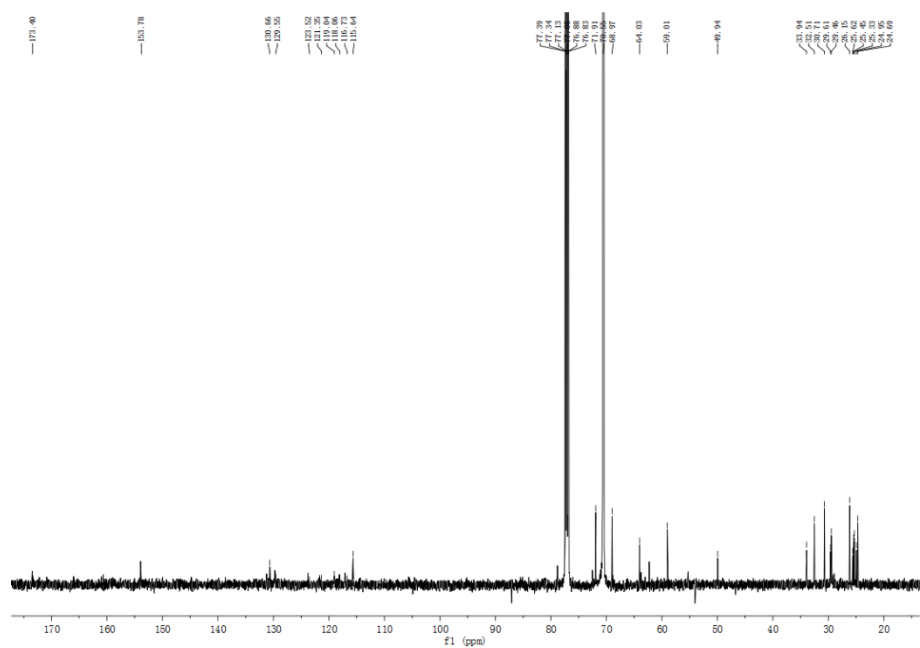


**Figure S5.**  $^{13}\text{C}$  NMR spectrum of PEGBAB in  $\text{CDCl}_3$ .

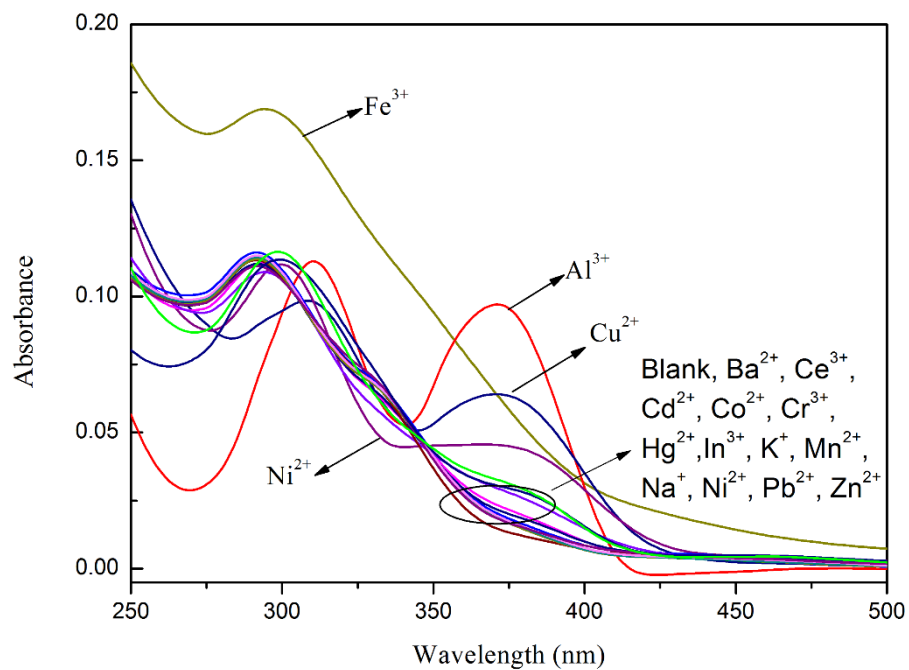


**Figure S6.** UV-Vis absorption spectra of PEGBAB (10  $\mu\text{M}$ ) with 2 equiv. of various metal ions in pure aqueous solutions.

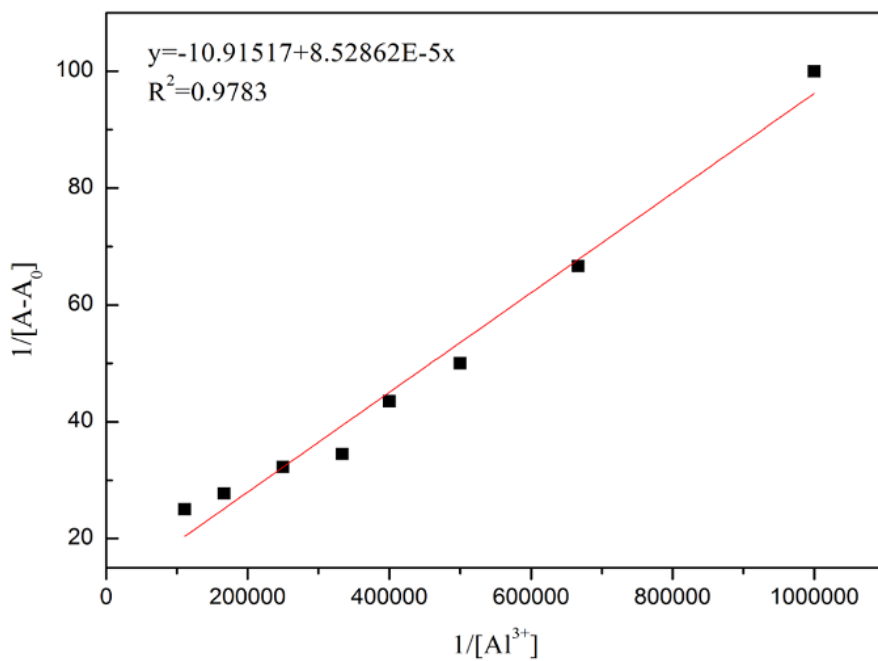


**Figure S7.** Benesi-Hildebrand plot of PEGBAB (10  $\mu\text{M}$ ) with  $\text{Al}^{3+}$  from UV-Vis titration profile for determination of association constant.

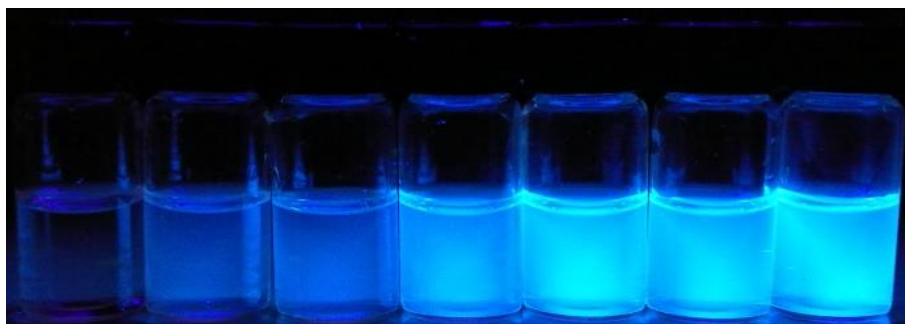


**Figure S8.** The photograph of PEGBAB (10  $\mu\text{M}$ ) in aqueous solution with different concentrations of  $\text{Al}^{3+}$  (from left to right: 0, 0.1, 0.25, 0.5, 1, 2, 5 equiv.) under a 365 nm UV lamp.

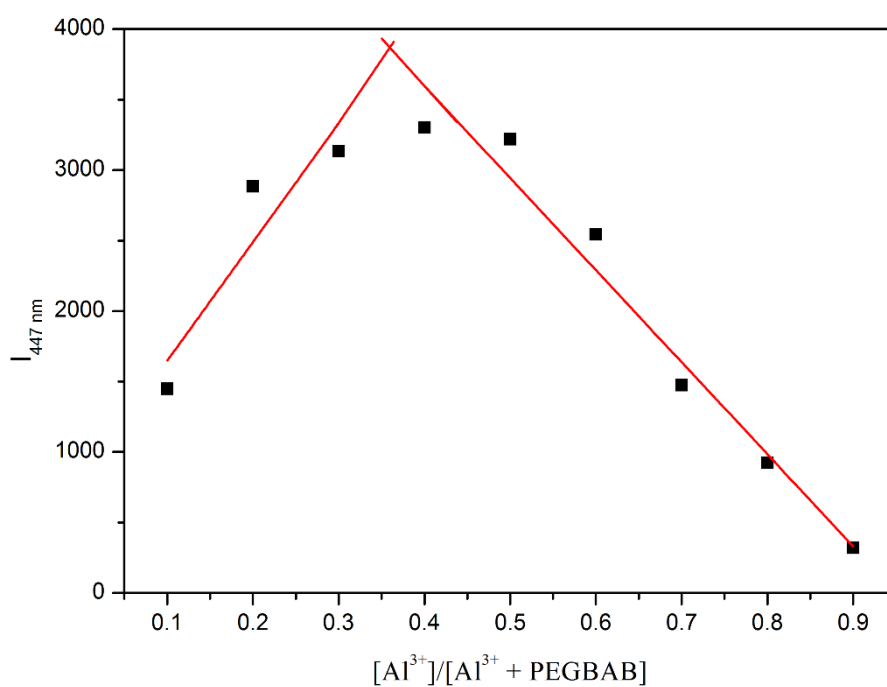


**Figure S9.** Job's plot of PEGBAB and  $\text{Al}^{3+}$  in aqueous solution. The total concentration of PEGBAB and  $\text{Al}^{3+}$  is 10  $\mu\text{M}$ .

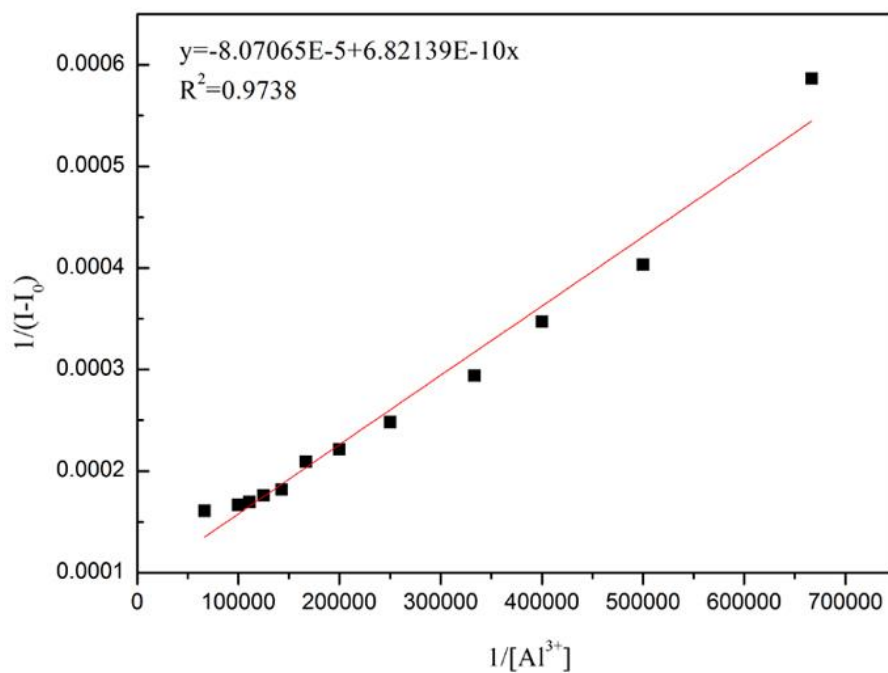


**Figure S10.** Benesi-Hildebrand plot of PEGBAB (10  $\mu$ M) with  $Al^{3+}$  from fluorescence titration profile for determination of association constant.

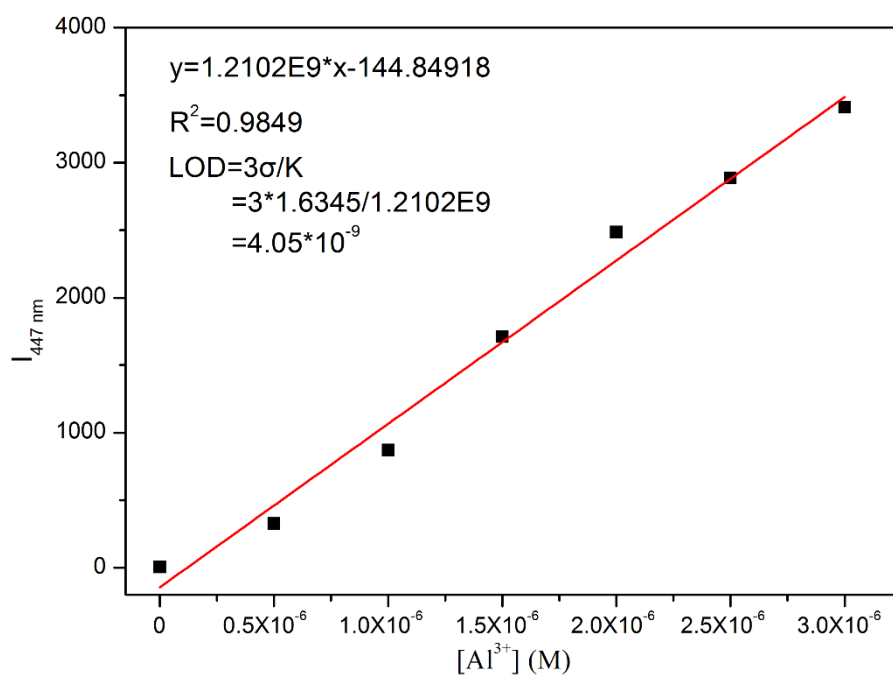


**Figure S11.** The linear of fluorescence intensity and concentration of  $Al^{3+}$  for the determination of limit of detection.

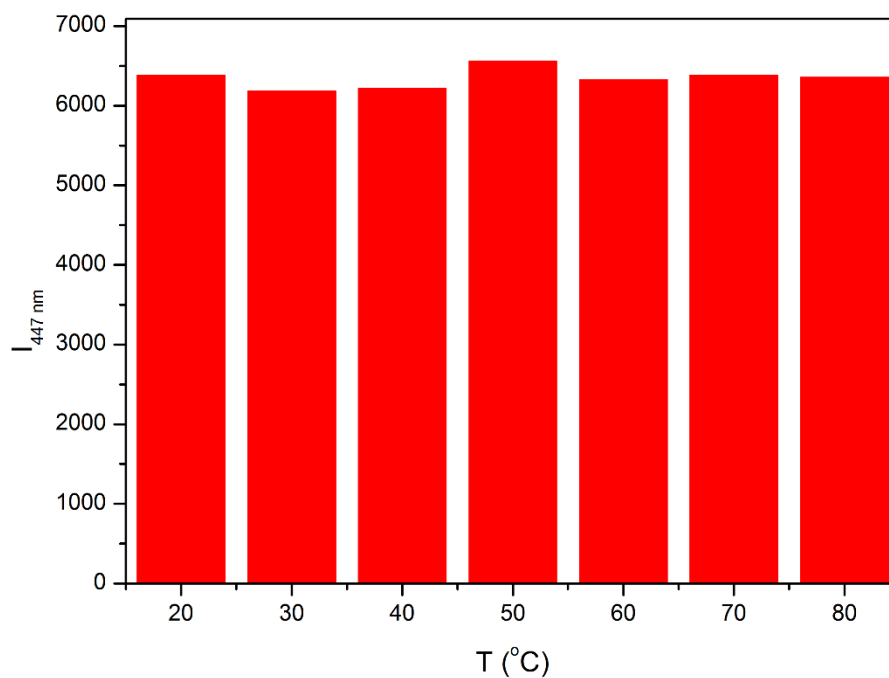


**Figure S12.** Effect of temperature on the fluorescence intensity at 447 nm of PEGBAB (10  $\mu$ M) in aqueous solutions upon addition of 2 equiv. of  $\text{Al}^{3+}$ .

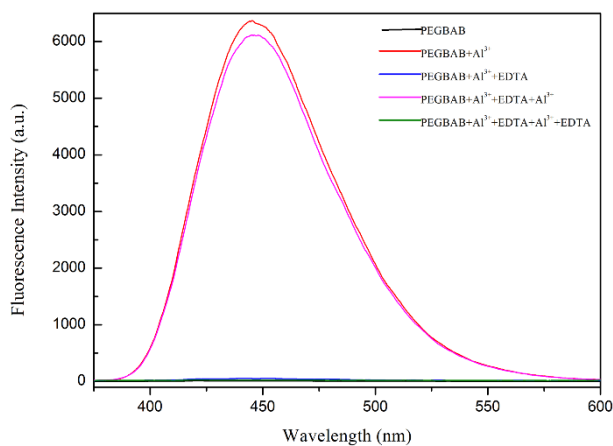


**Figure S13.** Fluorescence spectra of PEGBAB (10  $\mu$ M) in aqueous solution upon alternate addition of  $\text{Al}^{3+}$  (1 equiv.) and EDTA (1 equiv.).

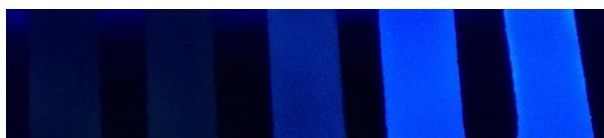


**Figure S14.** Photographs of test strips after being dipped into  $\text{Al}^{3+}$  solutions with different concentrations under a 365 nm UV lamp (from left to right:  $10^{-6}$  M,  $10^{-5}$  M,  $10^{-4}$  M,  $10^{-3}$  M,  $10^{-2}$  M).

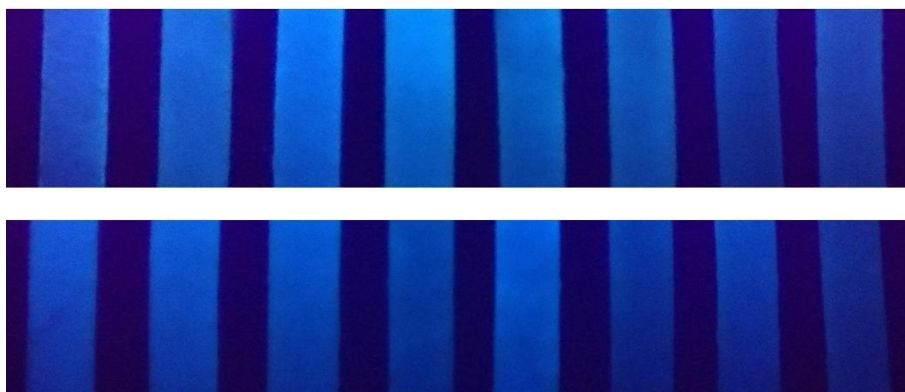


**Figure S15.** Photographs of test strips after being dipped into aqueous solutions of  $\text{Al}^{3+}$  (100  $\mu\text{M}$ ) mixed with different metal ions (100  $\mu\text{M}$ ) under a 365 nm UV lamp (from left to right, up:  $\text{Al}^{3+}$ ,  $\text{Ba}^{2+}$ ,  $\text{Ce}^{3+}$ ,  $\text{Cd}^{2+}$ ,  $\text{Co}^{2+}$ ,  $\text{Cr}^{3+}$ ,  $\text{Cu}^{2+}$  and  $\text{Fe}^{3+}$ ; down:  $\text{Hg}^{2+}$ ,  $\text{In}^{3+}$ ,  $\text{K}^+$ ,  $\text{Mn}^{2+}$ ,  $\text{Na}^+$ ,  $\text{Ni}^{2+}$ ,  $\text{Pb}^{2+}$  and  $\text{Zn}^{2+}$ ).

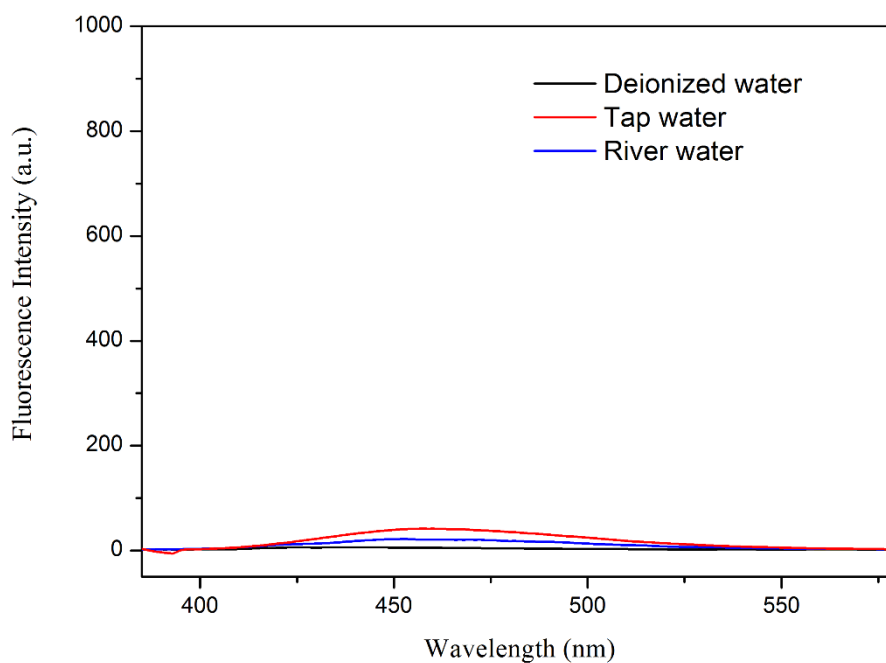


**Figure S16.** Fluorescence spectra of PEGBAB (10  $\mu\text{M}$ ) in different aqueous solution.



**Figure S17.** Photographs of test strips after being dipped into  $\text{Al}^{3+}$  solutions (100  $\mu\text{M}$ ) at different temperature under a 365 nm UV lamp (from left to right: 20 °C, 30 °C, 40 °C, 50 °C, 60 °C, 70 °C, 80 °C).



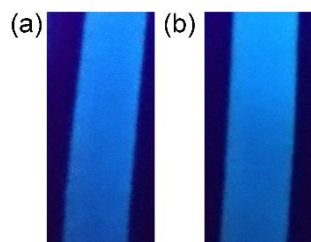


**Figure S18.** Photographs of test strips after being dipped into  $\text{Al}^{3+}$  solutions ( $100\ \mu\text{M}$ ) under a 365 nm UV lamp: (a) stored in air for 1 day; (b) stored in air for 7 days.